Received: 26 October 2021 | Revised: 5 April 2022 | Accepted: 10 April 2022

DOI: 10.1002/alz.12690

Alzheimer's & Dementia®
THE JOURNAL OF THE ALZHEIMER'S ASSOCIATION

FEATURED ARTICLE

Subcortical brain structures and the risk of dementia in the Rotterdam Study

Isabelle F. van der Velpen[1,2] | **Vanja Vlasov**[3] | **Tavia E. Evans**[2,4] | **Mohammad Kamran Ikram**[1,5] | **Boris A. Gutman**[6] | **Gennady V. Roshchupkin**[1,2] | **Hieab H. Adams**[2,4,7] | **Meike W. Vernooij**[1,2] | **Mohammad Arfan Ikram**[1]

[1]Department of Epidemiology, Erasmus MC University Medical Center, Rotterdam, the Netherlands

[2]Department of Radiology and Nuclear Medicine, Erasmus MC University Medical Center, Rotterdam, the Netherlands

[3]Interventional Neuroscience Group, Luxembourg Centre for Systems Biomedicine (LCSB), University of Luxembourg, Belvaux, Luxembourg

[4]Department of Clinical Genetics, Erasmus MC University Medical Center, Rotterdam, the Netherlands

[5]Department of Neurology, Erasmus MC University Medical Center, Rotterdam, the Netherlands

[6]Department of Biomedical Engineering, Illinois Institute of Technology, Chicago, Illinois, USA

[7]Latin American Brain Health (BrainLat), Universidad Adolfo Ibáñez, Santiago, Chile

Correspondence
Mohammad Arfan Ikram, Department of Epidemiology, Erasmus MC, PO Box 2040, 3000 CA Rotterdam, the Netherlands.
E-mail: m.a.ikram@erasmusmc.nl

Funding information
Erasmus Medical Center and Erasmus University; Research Institute for Diseases in the Elderly; Ministry of Education, Culture and Science; Ministry for Health, Welfare and Sports; The European Commission; Municipality of Rotterdam; Netherlands Organisation for Health Research and Development, Grant/Award Numbers: 733051082, 733050831, #73305095007

Abstract

Introduction: Volumetric and morphological changes in subcortical brain structures are present in persons with dementia, but it is unknown if these changes occur prior to diagnosis.

Methods: Between 2005 and 2016, 5522 Rotterdam Study participants (mean age: 64.4) underwent cerebral magnetic resonance imaging (MRI) and were followed for development of dementia until 2018. Volume and shape measures were obtained for seven subcortical structures.

Results: During 12 years of follow-up, 272 dementia cases occurred. Mean volumes of thalamus (hazard ratio [HR] per standard deviation [SD] decrease 1.94, 95% confidence interval [CI]: 1.55–2.43), amygdala (HR 1.66, 95% CI: 1.44–1.92), and hippocampus (HR 1.64, 95% CI: 1.43–1.88) were strongly associated with dementia risk. Associations for accumbens, pallidum, and caudate volumes were less pronounced. Shape analyses identified regional surface changes in the amygdala, limbic thalamus, and caudate.

Discussion: Structure of the amygdala, thalamus, hippocampus, and caudate is associated with risk of dementia in a large population-based cohort of older adults.

KEYWORDS
brain, dementia, epidemiology, magnetic resonance imaging, morphology, subcortical

1 | BACKGROUND

Worldwide, 50 million individuals currently live with dementia, a progressive neurodegenerative condition.[1] The disease usually clinically presents itself as cognitive impairment in several domains, including memory, executive function, language, and visuospatial abilities as well as changes in behavior or personality.[2] The underlying neurobiological correlates of these symptoms have typically been attributed to pathological changes and atrophy of the medial temporal lobe and cerebral cortex.[3] More recently, subcortical structures have been involved in dementia research.[4]

Subcortical brain structures comprise roughly 25% of human total brain volume and consist of a heterogeneous group of gray matter nuclei, including the thalamus, basal ganglia, hippocampus, amygdala, and nucleus accumbens.[4] These structures affect a wide array of physiological functions, including cognition, emotion regulation, motivation, and reward.[5] Against this background, several studies have shown how gross morphology of these structures is affected in persons with mild cognitive impairment (MCI) or dementia, possibly differentially across apolipoprotein E (*APOE*) ε4 carriers and non-carriers.[6–9] Although previous studies have mainly focused on volume of subcortical structures, their shape is thought to yield a deeper understanding of dementia neuropathology and symptoms.[10,11] In fact, one study showed how regional shape differences across persons provide meaningful insights into cognitive performance.[12]

Still, the number of studies on morphology of subcortical structures besides the hippocampus in the preclinical phase of dementia is limited.[13,14] Studying the subcortex would provide critical knowledge about the scope and localization of the neuropathological changes prior to dementia onset, which may then be targeted for disease monitoring or even possible intervention. In this study, we studied the association of volume and shape of subcortical brain structures with risk of dementia in community-dwelling older adults. We hypothesized that the shape of subcortical structures would show regional changes associated with dementia risk, independent of structure volume.

HIGHLIGHTS

- Volume and shape of subcortical structures are associated with dementia risk.
- Thalamus and amygdala volumes are related to incident dementia.
- Shape analyses reveal relevance of limbic thalamus for dementia risk.

RESEARCH IN CONTEXT

1. **Systematic Review**: The authors reviewed scientific literature using PubMed. The involvement of subcortical morphological changes and pathology have been previously described in study populations of persons with dementia. Recent publications in this field have increasingly focused on the shape of subcortical structures. These reports are appropriately cited.
2. **Interpretation**: Our findings indicate that subcortical brain structures are highly involved in dementia risk. The subcortical brain may be crucial to increase our understanding the complexity of dementia.
3. **Future Directions**: The role of subcortical brain structures in dementia should be included in further research on (1) etiology of dementia, (2) personalized prediction models for dementia onset, and (3) biological foundations of neuropsychiatric symptoms in early stages of dementia.

2 | METHODS

2.1 | Study population

This study was embedded in the Rotterdam Study, a population-based cohort study in the city of Rotterdam, the Netherlands.[15] Inhabitants of the neighborhood Ommoord were invited to participate in the study from 1990 onward. Participants were ≥45 years at baseline and were followed-up every 3 to 4 years. All participants provided written informed consent. The Rotterdam Study has been approved by the institutional review board (Medical Ethics Committee) of the Erasmus Medical Center and by the review board of the Dutch Ministry of Health, Welfare and Sports. All participants provided written informed consent to participate in the study.

Participants were invited for magnetic resonance imaging (MRI) of the brain from 2005 onward. Between August 2005 and August 2016, 5913 participants underwent a brain MRI. Follow-up data on dementia diagnosis was complete for 5820 of these participants (censored prior to MRI, $n = 27$; unusable follow-up data, $n = 66$). Participants with a dementia diagnosis at the time of the MRI scan ($n = 60$) were excluded from the study sample, leaving 5760 participants at risk to develop dementia. Participants with incomplete MRI image segmentation were excluded ($n = 238$). The final study sample comprised 5522 participants. Study baseline was determined by time of MRI, resulting in a baseline period from 2005 to 2013.

2.2 | Image acquisition and processing

MRI scanning of the brain was performed on a 1.5 Tesla MRI scanner (Signa Excite II, General Electric Healthcare) with an eight-channel head coil. The scan protocol included a T1-weighted sequence, proton density-weighted sequence, T2-weighted fluid attenuated inversion recovery (FLAIR) sequence, and 3D T2*-weighted gradient-recalled echo sequence. A detailed protocol of the Rotterdam Scan Study is described elsewhere.[16]

All scans were visually inspected by trained raters for image quality and evaluated for incidental findings. Cortical infarcts were rated on FLAIR, T1-weighted, and proton density-weighted sequences and were defined as focal parenchymal lesions with the same signal intensity as cerebrospinal fluid on all sequences and involvement of cortical gray matter, with a hyperintense rim on FLAIR images when located supratentorially.

Image processing was performed on the T1-weighted sequence (96 slices, slice thickness 1.6mm [zero padded to 0.8 mm], field of view 25 cm^2, matrix 416 × 256) using FreeSurfer (version 5.1) to obtain segmentation and volumetrics of subcortical structures.[17] Segmentations were obtained for the nucleus accumbens, amygdala, caudate, hippocampus, pallidum, putamen, and thalamus in each hemisphere. Global supratentorial gray matter volume was obtained by automated brain tissue segmentation based on a k-nearest neighbor (KNN) approach on T1-weighted images.[16] All KNN segmentations were visually inspected by trained raters and manually corrected when necessary.

Segmentations of subcortical structures were processed to obtain shape measures, using a previously described shape analysis pipeline.[18,19] In brief, a mesh model was created for the surface of each structure. Shape curvatures and medial features were matched to a precomputed template and registered using the "Medial Demons" framework.[20] For each individual surface model, a medial model was fit following Gutman et al.[21] Both medial and intrinsic features of the shape drive the registration to the precomputed template. The registration was performed in the fast spherical demons framework to minimize metric distortion.[22] Shape templates and mean medial curves were constructed previously and are distributed as part of the ENIGMA Shape package (http://enigma.ini.usc.edu/ongoing/enigma-shape-analysis/).

After processing, the resulting meshes for the 14 subcortical structures consist of a total of 27,120 vertices. Shape was quantified by two measures: the radial distance and the natural logarithm of the Jacobian determinant (Figure 1). The radial distance represents the distance from the medial curve to the vertex on the surface of the structure and as such denotes structure thickness. The Jacobian determinant represents the ratio of the subject-specific surface area relative to the template surface area and captures the shape deformation due to subregional volume change.[19] Positive values of the natural logarithm of the Jacobian determinant indicate a larger subregional volume (i.e., larger local surface area) of the subject-specific structure relative to the template. Negative values correspond to a smaller subregional volume (i.e., smaller local surface area) of the individual structure compared to the template.

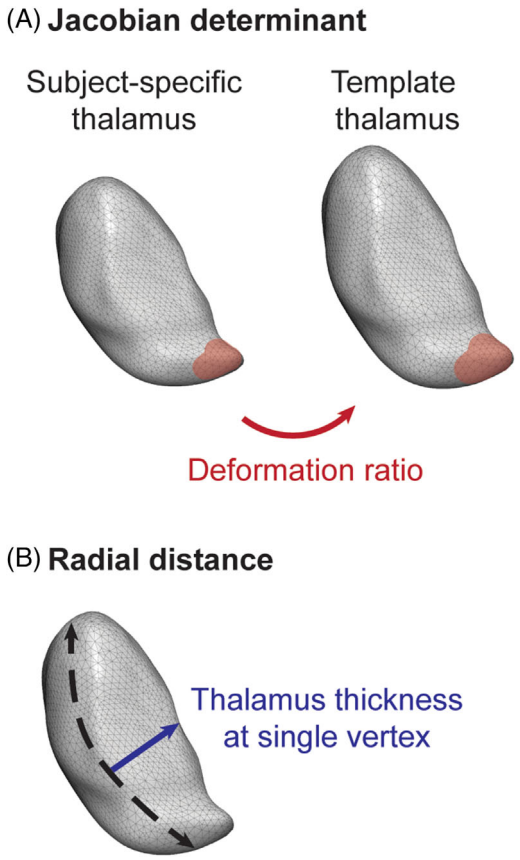

FIGURE 1 Methodological description of shape measures. Schematic overview of the derivation of shape measures. A, The Jacobian determinant represents the ratio of the subject-specific surface area relative to the template surface area and captures the shape deformation due to subregional volume change. Negative values correspond to a smaller subregional volume (i.e., smaller local surface area) of the individual structure compared to the template (depicted in red). Positive values of the natural logarithm of the Jacobian determinant indicate a larger subregional volume of the subject-specific structure relative to the template. B, The radial distance represents the distance from the medial curve to the vertex on the surface of the structure and as such denotes structure thickness. The medial curve of the thalamus is depicted by a dashed black line

2.3 | Assessment of dementia

All-cause dementia was the primary outcome in this study. Assessment of dementia was performed at baseline and each consecutive follow-up visit. During the visit to the research center, participants were screened for dementia with the Mini–Mental State Examination (MMSE) and the Geriatric Mental State Schedule (GMS) organic level. Participants with a MMSE < 26 or a GMS > 0 underwent an examination and informant interview with the Cambridge Examination for Mental Disorders of the Elderly (CAMDEX). Electronic linkage of the study database with medical records from general practitioners and the Regional Institute for Outpatient Mental Health Care provided additional continuous surveillance for dementia for the entire cohort.[23] A consensus panel led by a consultant neurologist decided on the final dementia diagnosis in all cases, in accordance with the Diagnostic and Statistical Manual of Mental Disorders III-R criteria for all-cause dementia and the National Institute of Neurological and Communicative Disorders and Stroke-Alzheimer's Disease and Related Disorders Association for the subtype of Alzheimer's disease (AD). Clinical neuroimaging was used as an aid to determine the

subtype of dementia or to rule out other causes when needed. Dementia follow-up was complete until January 1, 2018. Participants were censored at date of dementia diagnosis, death, loss to follow-up or January 1, 2018, whichever came first.

2.4 | Other measurements

Intracranial volume was obtained by automated MRI segmentation using FreeSurfer (version 5.1) as a proxy for head size.[17] Educational attainment was assessed during the baseline interview and was included as a covariate for its association with dementia and subcortical structures.[24] Depressive symptoms were assessed with the Center for Epidemiologic Studies–Depression scale (CES-D).[25] CES-D score at baseline was included as a covariate because of the association between depression and subcortical morphology, and depression and dementia.[26] *APOE* genotype was determined using polymerase chain reaction in the initial cohort of the Rotterdam Study, and with bi-allelic Taqman assay in two expansion cohorts of the Rotterdam Study. Participants were classified into carriers of the *APOE* ε4 allele (ε2/ε4, ε3/ε4, or ε4/ε4) and non-carriers (ε2/ε2, ε2/ε3, or ε3/ε3). Blood pressure was measured twice in sitting position using a random-zero sphygmomanometer at the research center, and mean blood pressure was calculated. Serum total cholesterol, high-density cholesterol, and fasting serum glucose levels were measured at the research center. A dummy variable was used to adjust for a proportion of glucose samples that were non-fasted. Use of psycholeptic or psychoanaleptic medication (Anatomical Therapeutic Chemical Classification code: N05 or N06) was based on self-report. The ascertainment of coronary heart disease and clinical stroke diagnoses was based on medical records and has been described in detail elsewhere.[15] Cerebral small vessel disease markers were defined as white matter hyperintensity (WMH) volume, presence of lacunar infarcts, and presence of cerebral microbleeds. WMH volume was obtained by automated brain tissue segmentation based on a KNN approach on T1-weighted and FLAIR images.[16] Lacunar infarcts were defined as focal lesions of noncortical tissue (size ≥3 and <15 mm), with the same signal intensity as cerebrospinal fluid on all sequences. Cerebral microbleeds were defined as focal areas of very low signal intensity on T2*-weighted gradient recalled echo images, which were not accompanied by signal abnormalities on other sequences.

2.5 | Statistical analyses

Missing covariate data (<1%) were imputed with 5-fold multiple imputation. Cox proportional hazard models were used to assess the risk of dementia associated with subcortical volume and shape. Time to dementia was modeled as continuous time in years. All analyses were adjusted for age, sex, total intracranial volume, education, CES-D score, systolic blood pressure, fasting blood glucose, total cholesterol, high-density cholesterol, psychotropic medication (psycholeptic and psychoanaleptic), presence of lacunar infarcts, presence of cerebral microbleeds, white matter hyperintensity volume, stroke, and coronary heart disease. Left, right, and mean subcortical volumes were standardized and used as main determinants in the volume analyses. In a separate model, we mutually adjusted all mean subcortical volumes and adjusted for global supratentorial gray matter volume. Correlation between subcortical structures was moderate (mean Pearson's $r = 0.56$, range 0.16–0.73). There was no multicollinearity in the mutually adjusted model. Analyses for mean subcortical volumes were then stratified on *APOE* ε4 carrier status. *APOE* ε4 homozygote and heterozygote carriers were grouped, due to limited power in the ε4/ε4 subgroup. Interaction was assessed by adding an interaction term of *APOE* ε4 carrier status with mean volume of each subcortical structure to the model. We additionally stratified volume analyses on sex and on time to dementia diagnosis (diagnosis within <3.5 years, 3.5–7.0 years, or >7.0 years of follow-up). Schoenfeld residuals were checked for the volume analyses; the proportional hazards assumption was not violated. A multiple testing correction for the main volume analyses was not applied, to prevent under-reporting on potentially relevant associations that future studies may further explore.

For shape analyses, the radial distance and Jacobian determinant for each vertex were used as independent variables, resulting in 54,240 models (radial distance and Jacobian determinant for 27,120 vertices). Shape measures were adjusted for gross volume of each subcortical structure in a separate model. Adjusting for both intracranial volume and gross structure volume did not result in multicollinearity. Shape analyses were subsequently stratified for *APOE* ε4 carrier status.

Vertex-wise measurements within and between subcortical structures may be correlated. We therefore determined the number of independent vertices per structure by permutation testing ($N = 10{,}000$), using a separate large population-based cohort. Linear regressions for radial distance and Jacobian determinant of all vertices were run with a random variable and repeated 10,000 times. The minimum *P*-value for each permutation was extracted and *P*-values were sorted to define the significance threshold based on the 5% quantile. Next, we divided 0.05 by this threshold to obtain the number of independent vertices per structure. The number of independent vertices within a structure was applied to calculate a structure-specific *P*-value threshold, using Šidák correction to control family-wise error.[27] The number of independent tests and *P*-value thresholds per structure are presented in Table SA.1 (Appendix A in supporting information). We additionally applied a stringent *P*-value threshold, based on the number of independent tests for all structures combined. The structure-specific *P*-threshold was adopted considering the shape analyses were informed by hypotheses based on the volumetric results, rather than using a completely hypothesis-free approach. Q-Q plots were used to inspect the distribution of expected and observed *P*-values around the structure-specific and stringent Šidák-corrected thresholds.

We performed four sensitivity analyses for volume and shape analyses: (1) with AD as outcome, (2) after exclusion of extreme outliers in subcortical volume (observations outside 2.5 x interquartile range [IQR]), (3) after exclusion of participants with cortical infarcts on MRI ($N = 203$), and (4) after exclusion of *APOE* ε2 carriers from the *APOE* ε4 stratified models. R package gaston was used for the Q-Q plots.[28]

TABLE 1 Baseline characteristics

	No dementia (*N* = 5250)	Incident dementia (*N* = 272)	Total sample (*N* = 5522)
Age (years), mean (SD)	63.7 (10.6)	76.3 (7.7)	64.4 (10.8)
Women, *N* (%)	2895 (55.1%)	164 (60.3%)	3059 (55.4%)
Education level, *N* (%)			
Primary education	452 (8.6%)	41 (15.1%)	493 (8.9%)
Lower/intermediate general or lower vocational	1991 (37.9%)	116 (42.6%)	2107 (38.2%)
Intermediate vocational or higher general	1601 (30.5%)	82 (30.1%)	1683 (30.5%)
Higher vocational education or university	1206 (23.0%)	33 (12.1%)	1239 (22.4%)
Depressive symptoms sum score (CES-D), median [IQR]	3.0 [1.0–6.0]	3.0 [1.0–6.0]	3.0 [1.0–6.0]
Clinically relevant depressive symptoms, *N* cases (%)	367 (7.0%)	18 (6.6%)	385 (7.0%)
Psycholeptics, *N* (%)	485 (9.2%)	31 (11.4%)	516 (9.3%)
Psychoanaleptics, *N* (%)	317 (6.0%)	25 (9.2%)	342 (6.2%)
Systolic blood pressure (mmHg), mean (SD)	140 (21.4)	149 (21.3)	140 (21.5)
Hypertension, *N* (%)	3317 (63.2%)	225 (82.7%)	3542 (64.1%)
Total cholesterol (mmol/L), mean (SD)	5.5 (1.1)	5.4 (1.1)	5.5 (1.1)
HDL cholesterol (mmol/L), mean (SD)	1.5 (0.4)	1.5 (0.4)	1.5 (0.4)
Glucose (mmol/L), mean (SD)	5.6 (1.2)	5.9 (1.3)	5.6 (1.2)
Fasting lab, *N* nonfasted (%)	103 (2.0%)	12 (4.4%)	115 (2.1%)
Diabetes mellitus, *N* (%)	650 (12.4%)	54 (19.9%)	704 (12.7%)
Coronary heart disease, *N* (%)	351 (6.7%)	28 (10.3%)	379 (6.9%)
Stroke, *N* (%)	151 (2.9%)	30 (11.0%)	181 (3.3%)
Apolipoprotein E ε4 heterozygote, *N* (%)	1307 (24.9%)	92 (33.8%)	1399 (25.3%)
Apolipoprotein E ε4 homozygote, *N* (%)	102 (1.9%)	16 (5.9%)	118 (2.1%)
Follow-up time from MRI scan onward (years), median [IQR]	9.2 [7.1–10.5]	5.4 [3.5–7.5]	9.1 [6.8–10.5]
Dementia diagnosis, *N* (%)			
Alzheimer's disease	-	205 (75.4%)	205 (3.7%)
Vascular dementia	-	6 (2.2%)	6 (0.1%)
Primary degenerative dementia (PDD)	-	3 (1.1%)	3 (0.1%)
Undetermined	-	46 (16.9%)	46 (0.8%)
Other	-	12 (4.4%)	12 (0.2%)
Imaging markers			
Intracranial volume (mL), mean (SD)	1480 (162)	1440 (170)	1480 (163)
Global gray matter volume (mL), mean (SD)	531 (61.6)	510 (59.8)	530 (61.7)
Cortical infarcts, *N* present (%)	180 (3.4%)	23 (8.5%)	203 (3.7%)
WMH volume (mL), median [IQR]	3.0 [1.7–6.2]	9.2 [4.3–19.8]	3.1 [1.7–6.7]
Lacunar infarcts, *N* present (%)	383 (7.3%)	45 (16.5%)	428 (7.8%)
Microbleeds, *N* present (%)	987 (18.8%)	106 (39.0%)	1093 (19.8%)
Left hemisphere subcortical structures (mL), mean (SD)			
Accumbens	0.56 (0.10)	0.51 (0.10)	0.56 (0.10)
Amygdala	1.32 (0.21)	1.16 (0.23)	1.31 (0.21)
Caudate	3.37 (0.52)	3.53 (0.72)	3.38 (0.54)
Hippocampus	3.88 (0.60)	3.34 (0.63)	3.86 (0.61)
Pallidum	1.49 (0.24)	1.33 (0.21)	1.48 (0.24)
Putamen	4.65 (0.65)	4.35 (0.78)	4.64 (0.66)
Thalamus	6.30 (0.78)	5.69 (0.64)	6.27 (0.79)

(Continues)

TABLE 1 (Continued)

	No dementia (*N* = 5250)	Incident dementia (*N* = 272)	Total sample (*N* = 5522)
Right hemisphere subcortical structures (mL), mean (SD)			
Accumbens	0.49 (0.10)	0.44 (0.10)	0.49 (0.10)
Amygdala	1.41 (0.21)	1.28 (0.24)	1.40 (0.22)
Caudate	3.49 (0.54)	3.66 (0.76)	3.50 (0.56)
Hippocampus	3.90 (0.56)	3.39 (0.55)	3.87 (0.57)
Pallidum	1.43 (0.25)	1.26 (0.22)	1.42 (0.25)
Putamen	4.49 (0.63)	4.21 (0.77)	4.48 (0.64)
Thalamus	6.31 (0.78)	5.68 (0.66)	6.28 (0.79)

Abbreviations: CES-D, Center for Epidemiologic Studies–Depression scale; HDL, high-density lipoprotein; IQR, interquartile range; MRI, magnetic resonance imaging; SD, standard deviation; WMH: white matter hyperintensity.

TABLE 2 Volume of subcortical structures and risk of dementia

	Hazard ratios with 95% confidence interval for risk of dementia (n/N = 272/5522)			
	Left hemisphere	Right hemisphere	Mean volumes	Mean volumes, mutually adjusted
Accumbens	1.29 (1.13–1.47)	1.23 (1.07–1.41)	1.31 (1.14–1.50)	1.22 (1.06–1.42)
Amygdala	1.42 (1.26–1.60)	1.46 (1.29–1.66)	1.66 (1.44–1.92)	1.31 (1.10–1.57)
Caudate	0.93 (0.83–1.04)	0.89 (0.79–0.99)	0.90 (0.81–1.01)	0.85 (0.74–0.98)
Hippocampus	1.36 (1.22–1.52)	1.41 (1.26–1.58)	1.64 (1.43–1.88)	1.35 (1.12–1.61)
Pallidum	1.28 (1.09–1.50)	1.32 (1.12–1.57)	1.37 (1.15–1.63)	1.06 (0.86–1.30)
Putamen	1.07 (0.94–1.22)	1.05 (0.92–1.19)	1.06 (0.93–1.22)	0.89 (0.76–1.05)
Thalamus	1.76 (1.42–2.18)	1.88 (1.51–2.33)	1.94 (1.55–2.43)	1.70 (1.32–2.18)

Note: Hazard ratio per standard deviation decrease of volume. Left, right, and mean volumes are adjusted for age, sex, total intracranial volume, education, Center for Epidemiologic Studies–Depression score, systolic blood pressure, fasting blood glucose, total cholesterol, high-density cholesterol, psychotropic medication (psycholeptic and psychoanaleptic), presence of lacunar infarcts, presence of cerebral microbleeds, white matter hyperintensity volume, stroke, and coronary heart disease. Mutually adjusted mean volumes were additionally adjusted for all other subcortical structures and supratentorial gray matter volume.
Abbreviations: n, number of cases; N, number of persons at risk.

3 | RESULTS

Baseline characteristics for 5522 participants are presented in Table 1. Mean age was 64.4 years and 3059 participants were female. During a follow-up of 46,661 person-years (median [IQR]: 9.1 years [6.8–10.5]), 272 participants developed dementia, of whom 205 were diagnosed with AD.

Volumes of all subcortical structures except the putamen were associated with dementia risk (Table 2). Associations were most pronounced for thalamus (hazard ratio [HR] per standard deviation [SD] decrease 1.94), amygdala (HR = 1.66), and hippocampus volumes (HR = 1.64). In the mutually adjusted model, all structures except the pallidum remained significantly associated with dementia risk. Larger caudate volume was associated with dementia risk (HR = 0.85). This finding was present in female participants, but not in males (Appendix A, Figure SA.1 in supporting information).

Accumbens and putamen volumes were associated with dementia risk in *APOE* ε4 non-carriers, but not in carriers (*P* for interaction = 0.004 in accumbens, *P* for interaction = 0.04 in putamen; Figure 2). There were no significant differences between *APOE* ε4 carriers and non-carriers for the other subcortical structures. Exclusion of *APOE* ε2 carriers did not change the results. Stratification on time to dementia diagnosis did not result in significant differences between groups (Appendix A, Figure SA.2 in supporting information).

Associations between subcortical shape and dementia risk are presented in Figure 3. Smaller subregional volume and thickness of the dorsal amygdala, dorsomedial and lateral thalamus, and medial and lateral hippocampus were associated with an increased dementia risk (Figure 3A–D). Larger subregional volume and thickness of the caudate tail was associated with a higher dementia risk, while the caudate head showed small clusters of lower thickness (Figure 3A–D). Shape changes were most widespread in the amygdala, where at most 27.3% of

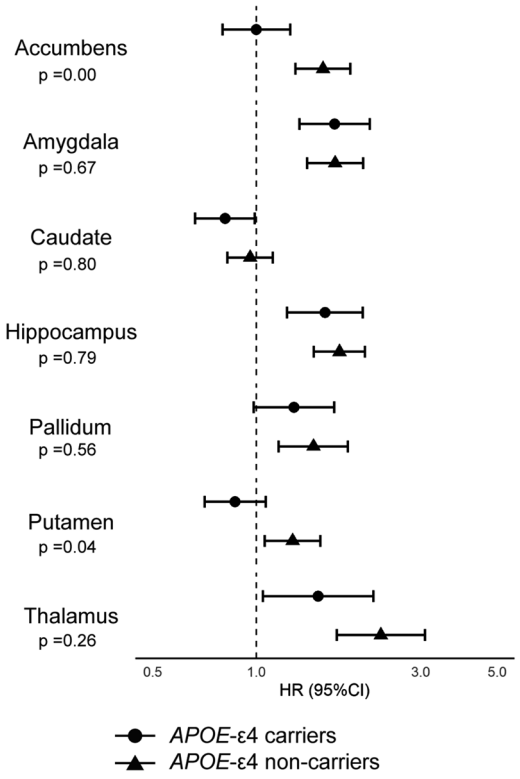

FIGURE 2 Volume of subcortical structures and risk of dementia for *APOE* ε4 carriers and non-carriers. Hazard ratio per standard deviation decrease of volume. *P* indicates *P*-value for the interaction term (mean structure volume x *APOE* ε4 carrier status). Incident dementia cases in *APOE* ε4 carriers group: 108/1517 (n/N). Incident dementia cases in *APOE* ε4 non-carriers group: 164/4005 (n/N). Models were adjusted for age, sex, total intracranial volume, education, CES-D score, systolic blood pressure, fasting blood glucose, total cholesterol, high-density cholesterol, psychotropic medication (psycholeptic and psychoanaleptic), presence of lacunar infarcts, presence of cerebral microbleeds, white matter hyperintensity volume, stroke, and coronary heart disease. Abbreviations: *APOE*, apolipoprotein E; CES-D, Center for Epidemiologic Studies–Depression; CI, confidence interval; HR, hazard ratio; n, number of cases; N, number of persons at risk

vertices was associated with dementia risk (Table 3, radial distance, right hemisphere). After adjusting for gross volume of each structure, most shape measures were no longer significantly associated with dementia risk (Figure 3E–H; Table 3). The lateral hippocampus and caudate tail demonstrated small clusters where larger subregional volume and thickness were associated with dementia.

Q-Q plots for shape measures show that the observed *P*-values overall were smaller than the expected *P*-values (Figure 3I). *P*-values above the Šidák-corrected significance thresholds are reported as significant findings. Small observed *P*-values below the *P*-value threshold indicate that more associations between shape and dementia risk are present, but likely remain undetected due to limited power. Differences in number of significant vertices between the structure-specific and stringent thresholds are small and do not change the interpretation of the findings.

Associations between subcortical structures and AD were similar to all-cause dementia (Tables SA.2 and SA.3 in supporting information). Associations between shape measures and dementia risk after stringent *P*-value correction are presented in Tables SA.4–A.5 and Figure SA.3 in supporting information. Shape analyses stratified for *APOE* ε4 carrier status did not show any differences between groups (data not shown). None of the sensitivity analyses changed the interpretation of the results.

4 | DISCUSSION

In this population-based study of older adults, amygdala, thalamus, hippocampus, and caudate structure was associated with dementia risk. Smaller overall volume of the thalamus, amygdala, and hippocampus was associated with incident dementia, accompanied by subregional volume loss and lower thickness. Larger caudate volume, localized in the caudate tail, was associated with dementia. After adjusting for structure-specific volume, associations between subcortical shape and dementia attenuated strongly.

We found that amygdala structure in dementia-free individuals was highly associated with dementia risk. This finding aligns with neuroimaging studies that showed amygdala atrophy in dementia patients.[9,29] Situated in the medial temporal lobe, the amygdala receives input from the sensory thalamus and cortex, and projects to prefrontal cortices, hippocampus, accumbens, hypothalamus, and brain stem.[30] Recent research indicates that both positive and negatives outcomes of behavior engage the amygdala, suggesting its function concerns valence-based learning, besides fear-conditioning alone.[30–32] Importantly, the amygdala is involved in processing social cues and guiding appropriate affective behavior.[33] Amygdala lesions impair innate and learned responses to social stimuli,[31] which may explain why patients with early-stage dementia demonstrate emotionally or socially inappropriate behaviors.[29] Our findings show that the amygdala contributes to dementia risk and may provide a basis for future studies on neural substrates of neuropsychiatric symptoms in cognitive decline.

Thalamus structure was strongly associated with dementia risk, with effect sizes for volume more pronounced than for hippocampus and amygdala. Shape changes were localized mainly to the limbic thalamus. To our knowledge, involvement of the thalamus in dementia risk has not been described before in a cognitively healthy sample. Previous studies have reported pathological changes in the thalamus in early stages of neurodegenerative diseases, and Braak and Braak found neurofibrillary changes in the limbic thalamus in the same stage as the hippocampus.[34–36] The anterior, mediodorsal, and laterodorsal nuclei have been termed the limbic thalamus due to their dense connections to other structures in the limbic system (e.g., hippocampus, amygdala, basal ganglia, and prefrontal cortex) and their involvement in cognitive function and emotion.[10,37] The role of the thalamus in cognitive function is increasingly established.[38,39] Current literature indicates that it is involved in executive functioning and memory processing,[37] potentially as a modulator of behavior-inducing

Alzheimer's & Dementia®
THE JOURNAL OF THE ALZHEIMER'S ASSOCIATION

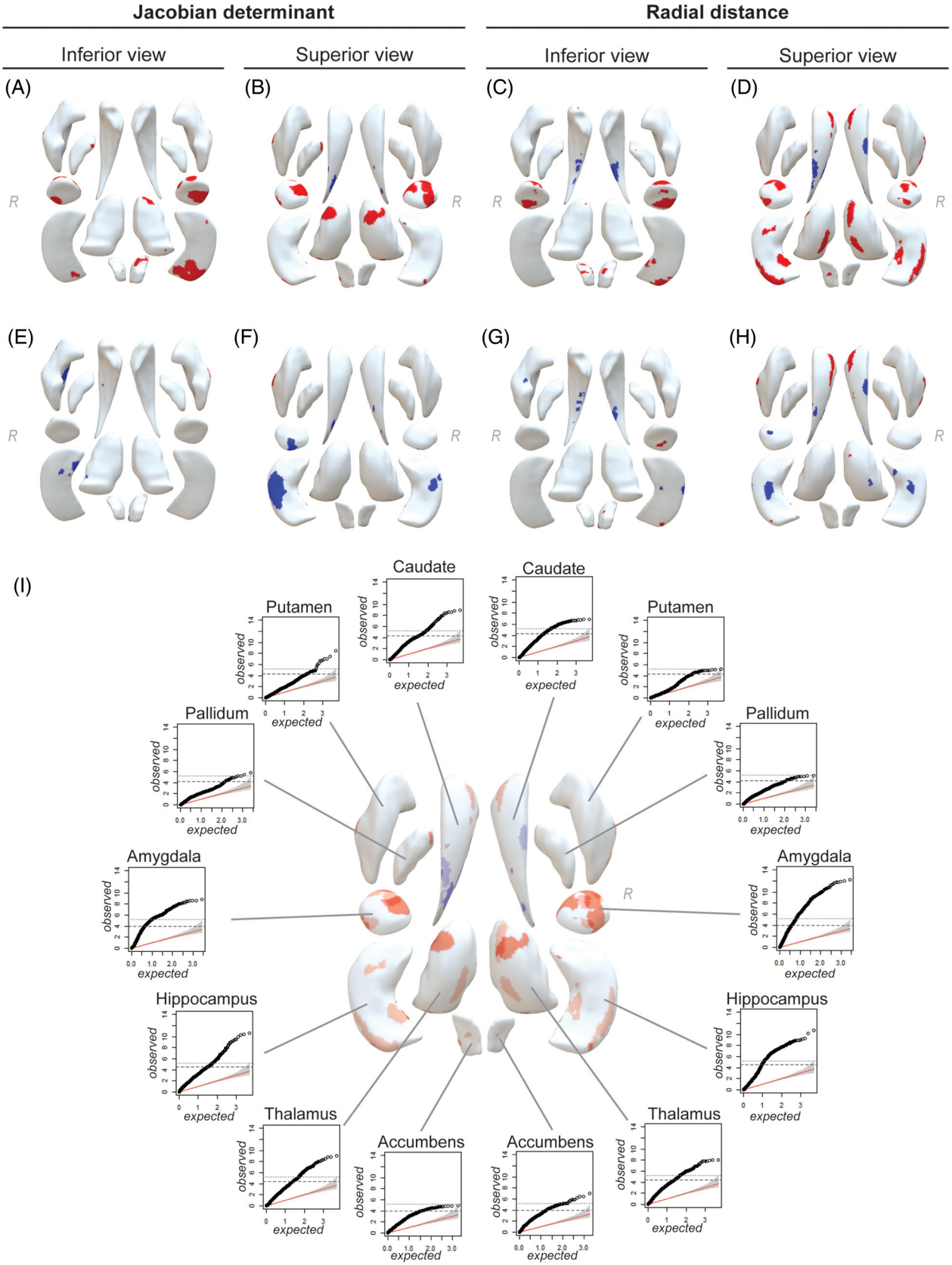

FIGURE 3 Dementia risk associated with shape measures of subcortical structures. Associations between subcortical shape measures and dementia are presented as red and blue surface areas for each structure. Red areas indicate that smaller subregional volume or thickness in a structure has an increased hazard ratio (HR) for dementia. Blue areas indicate that larger subregional volume or thickness of a structure has an increased HR for dementia. Only vertices with a statistically significant HR after Šidák correction are shown in red or blue. A–D, Model 1:

feedback to the cortex based on context information.[34,40] Combined with our findings, this indicates a central role for the thalamus in dementia pathology, likely contributing to early cognitive and emotional symptoms.

Unexpectedly, we found that larger caudate volume, mainly of the caudate tail, was associated with dementia risk. This finding was present in female, but not in male, participants. Larger caudate volumes have been described in AD compared to MCI patients, where this finding was partially explained by female sex and older age,[41] and in *PSEN1* mutation carriers in the prodromal phase of dementia.[42] In contrast, caudate atrophy has been associated with conversion from MCI to AD.[43] The caudate volume increase has been suggested as a temporary compensation for cognitive decline due to hippocampal atrophy in preclinical dementia, after which global atrophy may affect the caudate too.[41,44] Alternatively, measurement error through issues with image segmentation may explain these conflicting results. Longitudinal studies including imaging-trajectories before and after dementia diagnosis are needed to replicate and confirm our findings.

We found no differences between *APOE* ε4 carriers and non-carriers, except for accumbens and putamen volumes and dementia risk in non-carriers. This contrasts to previous studies in AD and MCI patients, which found that *APOE* ε4 carriers had more pronounced hippocampus, amygdala,[45,46] thalamus, and caudate volume loss than non-carriers.[8] A study in cognitively healthy adults reported altered microstructure of the thalamus in *APOE* ε4 carriers compared to non-carriers, but not in other subcortical structures.[47] Potentially, *APOE* ε4 carriers have different trajectories of subcortical changes after dementia diagnosis than prior to diagnosis.

The associations between shape and dementia risk attenuated strongly after adjusting for structure-specific volume, indicating that shape changes in this preclinical sample were explained mostly by gross volume. Still, shape measures demonstrate how gross volume changes are distributed across a structure, providing insight into localized morphological changes that volume measures alone do not identify. One study found that a prediction model for conversion from MCI to AD using subcortical shape was superior to a volume-based model.[48] Future research is needed to study the role of subcortical volume and shape in prediction of dementia in preclinical populations.

This study has several strengths and limitations. Strengths include the population-based design and neuroimaging in a preclinical setting, along with the use of several morphological markers. Although we were able to identify a substantial number of dementia cases, power in our stratified analyses for follow-up time and for shape in *APOE* ε4 carriers was too low to draw conclusions on morphological differences between subgroups. The findings from subgroup analyses should be interpreted with caution due to limited power. We did not apply a multiple testing correction for the volume analyses, to prevent under-reporting on potentially relevant associations. Finally, FreeSurfer has been reported to systematically overestimate subcortical volumes, which may have resulted in some general overestimation of our effect estimates, but not in differences between structures.[49,50]

In conclusion, subcortical structure, in particular of the amygdala and thalamus, is strongly related to dementia risk in a general population. The underlying etiology and resulting symptoms should be a focus of future research. Dementia is increasingly recognized as a complex multifactorial syndrome, with common early neuropsychiatric symptoms that warrant attention in addition to the cognitive symptoms, both in clinic and research. Although dementia research has traditionally had a strong focus on the hippocampus and neocortex, the subcortical brain may be crucial to increase our understanding the complexity of dementia.

ACKNOWLEDGMENTS

The Rotterdam Study is funded by Erasmus Medical Center and Erasmus University, Rotterdam, Netherlands Organization for the Health Research and Development (ZonMw); the Research Institute for Diseases in the Elderly (RIDE); the Ministry of Education, Culture and Science; the Ministry for Health, Welfare and Sports; the European Commission (DG XII); and the Municipality of Rotterdam. M.W. Vernooij is recipient of ABOARD, which is a public–private partnership receiving funding from ZonMW (#73305095007) and Health~Holland, Topsector Life Sciences & Health (PPP-allowance; #LSHM20106). This work was partially supported by the JPND project Social Health and Reserve in the Dementia patient journey (SHARED) and financed through projects funded by the Netherlands Organisation for Health Research and Development (grant numbers 733051082 and 733050831). Parts of this work were presented at the

associations adjusted for age, sex, total intracranial volume, education, CES-D score, systolic blood pressure, fasting blood glucose, total cholesterol, high-density cholesterol, psychotropic medication (psycholeptic and psychoanaleptic), presence of lacunar infarcts, presence of cerebral microbleeds, white matter hyperintensity volume, stroke, and coronary heart disease. E–H, Model 2: model 1 + adjusted for gross volume of each structure. I, Q-Q plots of the expected (x-axis) versus observed *P*-values (y-axis) for shape measures per subcortical structure. Red line with confidence interval represents theoretical χ^2-distrubution of expected *P*-values, corresponding to the null hypothesis. Black dots represent observed *P*-values for the associations between shape measures (Jacobian determinant and radial distance for each vertex are plotted together in each Q-Q plot) and dementia risk per subcortical structure. Horizontal gray dotted lines represent the – $\log_{10}$-transformed structure-specific *P*-value thresholds (bottom line) and stringent overall threshold (top line) for significant associations after Šidák correction. Separation of observed *P*-values from the red line toward the y-axis indicates deviation from the null hypothesis. The anatomical reference figure in (I) is a combination of (B) and (D), made transparent to show overlap in significant clusters for both Jacobian determinant and radial distance. R indicates hemispherical orientation

TABLE 3 Shape of subcortical structures and dementia risk

		Jacobian determinant				Radial distance			
Left hemisphere	**Total**	**Mod.**	**Min. *P***	**#Pos, N (%)**	**#Neg, N (%)**	**Mod.**	**Min. *P***	**#Pos, N (%)**	**#Neg, N (%)**
Accumbens	930	1	$5.36*10^{-5}$	0 (0.0)	3 (0.3)	1	$1.04*10^{-5}$	0 (0.0)	42 (4.5)
		2	$8.85*10^{-3}$	0 (0.0)	0 (0.0)	2	$4.23*10^{-3}$	0 (0.0)	0 (0.0)
Amygdala	1368	1	$1.57*10^{-9}$	0 (0.0)	372 (27.2)	1	$2.39*10^{-9}$	0 (0.0)	220 (16.1)
		2	$8.92*10^{-5}$	3 (0.2)	0 (0.0)	2	$1.47*10^{-4}$	0 (0.0)	0 (0.0)
Caudate	2502	1	$1.93*10^{-5}$	10 (0.4)	0 (0.0)	1	$9.97*10^{-10}$	81 (3.2)	56 (2.2)
		2	$1.26*10^{-5}$	11 (0.4)	0 (0.0)	2	$9.20*10^{-10}$	70 (2.8)	71 (2.8)
Hippocampus	2502	1	$7.57*10^{-6}$	0 (0.0)	32 (1.3)	1	$2.57*10^{-11}$	0 (0.0)	140 (5.6)
		2	$5.71*10^{-6}$	85 (3.4)	0 (0.0)	2	$6.63*10^{-8}$	40 (1.6)	0 (0.0)
Pallidum	1254	1	$1.63*10^{-6}$	0 (0.0)	13 (1.0)	1	$1.27*10^{-5}$	0 (0.0)	4 (0.3)
		2	$1.25*10^{-4}$	0 (0.0)	0 (0.0)	2	$3.56*10^{-4}$	0 (0.0)	0 (0.0)
Putamen	2502	1	$1.42*10^{-5}$	0 (0.0)	8 (0.3)	1	$3.21*10^{-9}$	0 (0.0)	27 (1.1)
		2	$6.05*10^{-7}$	47 (1.9)	6 (0.2)	2	$6.26*10^{-10}$	8 (0.3)	35 (1.4)
Thalamus	2502	1	$1.19*10^{-7}$	0 (0.0)	78 (3.1)	1	$7.78*10^{-10}$	0 (0.0)	120 (4.8)
		2	$1.16*10^{-5}$	5 (0.2)	0 (0.0)	2	$1.01*10^{-5}$	7 (0.3)	3 (0.1)
Right hemisphere		**Jacobian determinant**				**Radial distance**			
	Total	**Mod.**	**Min. *P***	**#Pos, N (%)**	**#Neg, N (%)**	**Mod.**	**Min. *P***	**#Pos, N (%)**	**#Neg, N (%)**
Accumbens	930	1	$5.93*10^{-6}$	0 (0.0)	62 (6.7)	1	$9.65*10^{-8}$	4 (0.4)	34 (3.7)
		2	$1.77*10^{-5}$	5 (0.5)	0 (0.0)	2	$8.54*10^{-6}$	11 (1.2)	4 (0.4)
Amygdala	1368	1	$6.76*10^{-11}$	0 (0.0)	317 (23.2)	1	$5.72*10^{-13}$	0 (0.0)	374 (27.3)
		2	$3.66*10^{-8}$	91 (6.7)	0 (0.0)	2	$2.29*10^{-7}$	12 (0.9)	17 (1.2)
Caudate	2502	1	$1.74*10^{-7}$	60 (2.4)	0 (0.0)	1	$1.20*10^{-7}$	152 (6.1)	39 (1.6)
		2	$1.23*10^{-6}$	26 (1.0)	0 (0.0)	2	$4.28*10^{-7}$	56 (2.2)	70 (2.8)
Hippocampus	2502	1	$1.10*10^{-9}$	0 (0.0)	246 (9.8)	1	$1.70*10^{-11}$	0 (0.0)	312 (12.5)
		2	$1.94*10^{-9}$	191 (7.6)	0 (0.0)	2	$1.45*10^{-10}$	77 (3.1)	11 (0.4)
Pallidum	1254	1	$8.16*10^{-6}$	0 (0.0)	20 (1.6)	1	$5.06*10^{-5}$	0 (0.0)	1 (0.1)
		2	$1.53*10^{-3}$	0 (0.0)	0 (0.0)	2	$1.62*10^{-3}$	0 (0.0)	0 (0.0)
Putamen	2502	1	$7.53*10^{-6}$	0 (0.0)	29 (1.2)	1	$6.46*10^{-6}$	0 (0.0)	4 (0.2)
		2	$8.17*10^{-7}$	0 (0.0)	48 (1.9)	2	$2.91*10^{-6}$	0 (0.0)	23 (0.9)
Thalamus	2502	1	$1.14*10^{-7}$	0 (0.0)	114 (4.6)	1	$8.55*10^{-9}$	0 (0.0)	82 (3.3)
		2	$6.67*10^{-4}$	0 (0.0)	0 (0.0)	2	$1.43*10^{-4}$	0 (0.0)	0 (0.0)

Note: Number of vertices that are significantly associated with dementia risk in Cox proportional hazard models. Structure-specific *P*-value thresholds for significant associations after Šidák correction were: accumbens $9.18*10^{-5;}$ amygdala $9.00*10^{-5}$; caudate $5.02*10^{-5}$; hippocampus $3.26*10^{-5}$; pallidum $6.53*10^{-5}$; putamen $4.95*10^{-5}$; thalamus $3.82*10^{-5}$. Total, total number of vertices per structure; Mod, model; Min. *P*, lowest *P*-value for each structure; #Pos, number of vertices with a statistically significant positive association with the outcome, indicating that an increase in the measure (larger subregional volume or thickness) is associated with a higher dementia risk; #Neg, number of vertices with a statistically significant negative association with the outcome, indicating that a decrease in the measure (smaller subregional volume or thickness) is associated with an increased dementia risk.

Model 1: adjusted for age, sex, total intracranial volume, education, Center for Epidemiologic Studies–Depression score, systolic blood pressure, fasting blood glucose, total cholesterol, high-density cholesterol, psychotropic medication (psycholeptic and psychoanaleptic), presence of lacunar infarcts, presence of cerebral microbleeds, white matter hyperintensity volume, stroke, and coronary heart disease.

Model 2: model 1 + adjusted for gross volume of each structure.

2017 Alzheimer's Association International Conference; no abstract or other information was published previously. The authors are grateful to the study participants, the staff from the Rotterdam Study, and the participating general practitioners and pharmacists.

CONFLICTS OF INTEREST

The authors declare that there are no conflicts of interest.

REFERENCES

1. Livingston G, Huntley J, Sommerlad A, et al. Dementia prevention, intervention, and care: 2020 report of the Lancet Commission. *Lancet*. 2020;396:413–446.
2. Arvanitakis Z, Shah RC, Bennett DA. Diagnosis and management of dementia: review. *JAMA*. 2019;322:1589–1599.
3. Elahi FM, Miller BL. A clinicopathological approach to the diagnosis of dementia. *Nat Rev Neurol*. 2017;13:457–476.
4. Forstmann BU, de Hollander G, van Maanen L, Alkemade A, Keuken MC. Towards a mechanistic understanding of the human subcortex. *Nat Rev Neurosci*. 2017;18:57–65.
5. Tate DF, Wade BSC, Velez CS, et al. Subcortical shape and neuropsychological function among U.S. service members with mild traumatic brain injury. *Brain Imaging Behav*. 2019;13:377–388.
6. Cho H, Kim JH, Kim C, et al. Shape changes of the basal ganglia and thalamus in Alzheimer's disease: a three-year longitudinal study. *J Alzheimers Dis*. 2014;40:285–295.
7. Leh SE, Kalin AM, Schroeder C, et al. Volumetric and shape analysis of the thalamus and striatum in amnestic mild cognitive impairment. *J Alzheimers Dis*. 2016;49:237–249.
8. Novellino F, López ME, Vaccaro MG, Miguel Y, Delgado ML, Maestu F. Association between hippocampus, thalamus, and caudate in mild cognitive impairment APOEε4 carriers: a structural covariance MRI study. *Front Neurol*. 2019;10:1303.
9. Wachinger C, Salat DH, Weiner M, Reuter M, Alzheimer's Disease Neuroimaging I. Whole-brain analysis reveals increased neuroanatomical asymmetries in dementia for hippocampus and amygdala. *Brain*. 2016;139:3253–3266.
10. Zonneveld HI, Roshchupkin GV, Adams HHH, et al. High-dimensional mapping of cognition to the brain using voxel-based morphometry and subcortical shape analysis. *J Alzheimers Dis*. 2019;71:141–152.
11. Rahayel S, Bocti C, Sévigny Dupont P, et al. Subcortical amyloid load is associated with shape and volume in cognitively normal individuals. *Hum Brain Mapp*. 2019;40:3951–3965.
12. Seidl U, Traeger TV, Hirjak D, et al. Subcortical morphological correlates of impaired clock drawing performance. *Neurosci Lett*. 2012;512:28–32.
13. Hilal S, Amin SM, Venketasubramanian N, et al. Subcortical atrophy in cognitive impairment and dementia. *J Alzheimers Dis*. 2015;48:813–823.
14. de Jong LW, Wang Y, White LR, Yu B, van Buchem MA, Launer LJ. Ventral striatal volume is associated with cognitive decline in older people: a population based MR-study. *Neurobiol Aging*. 2012;33:424 e1–10xs.
15. Ikram MA, Brusselle G, Ghanbari M, et al. Objectives, design and main findings until 2020 from the Rotterdam Study. *Eur J Epidemiol*. 2020;35:483–517.
16. Ikram MA, van der Lugt A, Niessen WJ, et al. The Rotterdam Scan Study: design update 2016 and main findings. *Eur J Epidemiol*. 2015;30:1299–1315.
17. Fischl B, Salat DH, van der Kouwe AJ, et al. Sequence-independent segmentation of magnetic resonance images. *Neuroimage*. 2004;23 Suppl 1:S69–S84.
18. Gutman BA, Fletcher PT, Cardoso MJ, et al. A Riemannian framework for intrinsic comparison of closed genus-zero shapes. *Inf Process Med Imaging*. 2015;24:205–218.
19. Roshchupkin GV, Gutman BA, Vernooij MW, et al. Heritability of the shape of subcortical brain structures in the general population. *Nat Commun*. 2016;7:13738.
20. Gutman BA, Hua X, Rajagopalan P, et al. Maximizing power to track Alzheimer's disease and MCI progression by LDA-based weighting of longitudinal ventricular surface features. *Neuroimage*. 2013;70:386–401.
21. Gutman BA, Jahanshad N, Ching CR, et al. Medial demons registration localizes the degree of genetic influence over subcortical shape variability: an N = 1480 meta-analysis. *Proc IEEE Int Symp Biomed Imaging*. 2015; Apr.:1402–1406.
22. Gutman BA, Madsen SK, Toga AW, Thompson PM. *A Family of Fast Spherical Registration Algorithms for Cortical Shapes*. In: Shen, L, Liu, T, Yap, PT, Huang, H, Shen, D, Westin, CF. (eds) Multimodal Brain Image Analysis. MBIA 2013. Lecture Notes in Computer Science, vol 8159. Cham: Springer International Publishing; 2013: 246–257.
23. Ott A, Breteler MM, van Harskamp F, Stijnen T, Hofman A. Incidence and risk of dementia. the Rotterdam Study. *Am J Epidemiol*. 1998;147:574–580.
24. Tang X, Varma VR, Miller MI, Carlson MC. Education is associated with sub-regions of the hippocampus and the amygdala vulnerable to neuropathologies of Alzheimer's disease. *Brain Struct Funct*. 2017;222:1469–1479.
25. Radloff LS. The CES-D Scale: a self-report depression scale for research in the general population. *Appl Psycholo Meas*. 1977;1:385–401.
26. Ho TC, Gutman B, Pozzi E, et al. Subcortical shape alterations in major depressive disorder: findings from the ENIGMA major depressive disorder working group. *Hum Brain Mapp*. 2022;43(1): 341–351.
27. Sidak Z. Rectangular confidence regions for the means of multivariate normal distributions. *J Am Stat Assoc*. 1967;62:626–633.
28. Dandine-Roulland C, Perdry H. *Genome-Wide Data Manipulation, Association Analysis and Heritability Estimates in R with Gaston 1.5*. In: Heredity H, ed. 46th European Mathematical Genetics Meeting (EMGM); 2018. Cagliari, Italy, April 18-20, 2018: Abstracts 2018. p. 1–29.
29. Poulin SP, Dautoff R, Morris JC, Barrett LF, Dickerson BC, Alzheimer's Disease Neuroimaging I. Amygdala atrophy is prominent in early Alzheimer's disease and relates to symptom severity. *Psychiatry Res*. 2011;194:7–13.
30. Janak PH, Tye KM. From circuits to behaviour in the amygdala. *Nature*. 2015;517:284–292.
31. O'Neill PK, Gore F, Salzman CD. Basolateral amygdala circuitry in positive and negative valence. *Curr Opin Neurobiol*. 2018;49:175–183.
32. Yang Y, Wang JZ. From structure to behavior in basolateral amygdala-hippocampus circuits. *Front Neural Circuits*. 2017;11:86.
33. Feldman R. The neurobiology of human attachments. *Trends Cogn Sci*. 2017;21:80–99.
34. Power BD, Looi JC. The thalamus as a putative biomarker in neurodegenerative disorders. *Aust N Z J Psychiatry*. 2015;49:502–518.
35. Aggleton JP, Pralus A, Nelson AJ, Hornberger M. Thalamic pathology and memory loss in early Alzheimer's disease: moving the focus from the medial temporal lobe to Papez circuit. *Brain*. 2016;139:1877–1890.
36. Braak H, Braak E. Alzheimer's disease affects limbic nuclei of the thalamus. *Acta Neuropathol*. 1991;81:261–268.
37. Georgescu IA, Popa D, Zagrean L. The anatomical and functional heterogeneity of the mediodorsal thalamus. *Brain Sci*. 2020;10(9):624. https://doi.org/10.3390/brainsci10090624
38. Weaver NA, Kuijf HJ, Aben HP, et al. Strategic infarct locations for post-stroke cognitive impairment: a pooled analysis of individual patient data from 12 acute ischaemic stroke cohorts. *Lancet Neurol*. 2021;20:448–459.

39. Cremers LG, de Groot M, Hofman A, et al. Altered tract-specific white matter microstructure is related to poorer cognitive performance: the Rotterdam Study. *Neurobiol Aging*. 2016;39:108–117.
40. Rikhye RV, Wimmer RD, Halassa MM. Toward an integrative theory of thalamic function. *Annu Rev Neurosci*. 2018;41:163–183.
41. Persson K, Bohbot VD, Bogdanovic N, Selbaek G, Braekhus A, Engedal K. Finding of increased caudate nucleus in patients with Alzheimer's disease. *Acta Neurol Scand*. 2018;137:224–232.
42. Lee GJ, Lu PH, Medina LD, et al. Regional brain volume differences in symptomatic and presymptomatic carriers of familial Alzheimer's disease mutations. *J Neurol Neurosurg Psychiatry*. 2013;84:154–162.
43. Tuokkola T, Karrasch M, Koikkalainen J, et al. Association between deep gray matter changes and neurocognitive function in mild cognitive impairment and Alzheimer's disease: a tensor-based morphometric MRI study. *Dement Geriatr Cogn Disord*. 2019;48:68–78.
44. Le Floch M, Ali P, Asfar M, Sánchez-Rodríguez D, Dinomais M, Annweiler C. Volumetric brain changes in older fallers: a voxel-based morphometric study. *Front Bioeng Biotechnol*. 2021;9:610426. Published 2021 Mar 10. https://doi.org/10.3389/fbioe.2021.610426
45. Lupton MK, Strike L, Hansell NK, et al. The effect of increased genetic risk for Alzheimer's disease on hippocampal and amygdala volume. *Neurobiol Aging*. 2016;40:68–77.
46. Zhang C, Kong M, Wei H, et al. The effect of ApoE ε 4 on clinical and structural MRI markers in prodromal Alzheimer's disease. *Quant Imaging Med Surg*. 2020;10:464–474.
47. Mole JP, Fasano F, Evans J, et al. APOE-ε4-related differences in left thalamic microstructure in cognitively healthy adults. *Sci Rep*. 2020;10:19787.
48. Tang X, Holland D, Dale AM, Younes L, Miller MI. Baseline shape diffeomorphometry patterns of subcortical and ventricular structures in predicting conversion of mild cognitive impairment to Alzheimer's disease. *J Alzheimers Dis*. 2015;44:599–611.
49. Srinivasan D, Erus G, Doshi J, et al. A comparison of Freesurfer and multi-atlas MUSE for brain anatomy segmentation: Findings about size and age bias, and inter-scanner stability in multi-site aging studies. *Neuroimage*. 2020;223:117248.
50. Fraser MA, Shaw ME, Anstey KJ, Cherbuin N. Longitudinal assessment of hippocampal atrophy in midlife and early old age: contrasting manual tracing and semi-automated segmentation (FreeSurfer). *Brain Topogr*. 2018;31:949–962.

SUPPORTING INFORMATION

Additional supporting information can be found online in the Supporting Information section at the end of this article.

How to cite this article: van der Velpen IF, Vlasov V, Evans TE, et al. Subcortical brain structures and the risk of dementia in the Rotterdam Study. *Alzheimer's Dement*. 2023;19:646–657. https://doi.org/10.1002/alz.12690